Annals of R.S.C.B., ISSN:1583-6258, Vol. 25, Issue 5, 2021, Pages. 3282–3290
Received 15 April 2021; Accepted 05 May 2021

Integration of 2D seismic data interpretation and seismic attributes to delineate the subsurface configurations in Ras Gara area, southern Gulf of Suez, Egypt

A. Ghoneimi[a], A. El-Khadragy[a], A. Alaa Eldin[b], A. Azab[b]
[a] Geology Department, Faculty of Science, Zagazig University, Egypt
[b] Exploration Department, Egyptian Petroleum Research Institute, Cairo
Corresponding author email: ahmedalaaeldin93@hotmail.com

Abstract: A grid of 2D marine seismic lines was interpreted and treated with seismic attributes to delineate the subsurface structures and disclose the hidden features. The ordinary steps of seismic reflection analysis were carried out to get meaningful images of Miocene. structures through constructing a set of two-way time structure maps for five targets. In addition, the seismic attribute enhancement procedures were implemented to best visualize salt/subsalt source structures. Both of structural and stratigraphic types of seismic attributes were applied on time migrated seismic sections to allow significant improvements in the fault detection and geometry of the strata. The results of seismic interpretation indicate presence of a salt diaper on top of South Gharib Formation, underlain by a Pre-Mio. (PM) uplift and flanked by dipping limbs to the east and west. The subsalt section is deformed by NW-SE (Clysmic) faults, which inherited from old fractures on top of basement along lines of weakness. The inner structure of the block exhibits a lack of the NE-SW-trending (cross-gulf) faults. The structural attributes highlight numerous hairline fractures of small displacements disturb the Pre-Miocene section and reduced in number at the Miocene level. The stratigraphic attributes filters succeeded to delimit lithological boundaries changes, trace salt contacts, and define "bright spots" with respect to hydrocarbon reservoirs. Generally, the dip-reversals along the diapir flanks and limbs of the PM uplift are believed to be the most potential traps.
Keywords: Gulf of Suez; Ras Gara; Seismic attributes; Applied geophysics; Salt diaper.

1. Introduction

The Gulf of Suez rift is the oldest productive region in Egypt and has a long history of hydrocarbons exploration. It is characterized by an intricate structure and lithology and contains many concessions and oil fields, particularly in the central and southern parts. The hydrocarbons reserves discovered in the southern gulf are lithologically related to Miocene (Mio.) and PM reservoirs **[1]** and structurally are closely associated with tilted fault blocks **[2]**. The prospective blocks are delimited from north and south by NE-SW Aqaba faults and from east and west by NW-SE Clysmic faults **[3]** and delineate most oil fields **[4]**. At Mio. level, mapping of these cross-faults and related structures is reliable and avail from the seismic reflection. But, it is very difficult to image details at PM level, due to low seismic resolutions because of the seismic reflectivity is not good. This blind zone on seismic sections is largely due to the thick laminated evaporite section that often conceals deep signals. The strong shielding and lamination of the

Annals of R.S.C.B., ISSN:1583-6258, Vol. 25, Issue 5, 2021, Pages. 3282–3290
Received 15 April 2021; Accepted 05 May 2021

evaporitic rocks led to lack of deeper reflectors. The attenuation and dispersion of seismic P-waves are maximized with the Mio. salt structures. As a result, many of the exploratory wells drilled below the Mio. evaporites are mostly dry holes.

In the study area, the thick salt section of South Gharib (SG) Fm. is considered as a double-edged sword. It makes as good seal for any hydrocarbon migrations, and constitutes problems for the deep seismic interpretation. The problem has encountered in determining the structure and stratigraphic boundaries of PM horizons where the data become poor. Therefore, the seismic attributes could be used in characterizing the geological details including; salt geometry, salt-flanks, subsalt structure and to predict reservoir location in the salt basins. It may be effective in locating new prospects for drilling or guide evolution of the already discovered fields.

The most common attributes are those ones obtained from post-stack seismic reflection. Such attribute computations act as filters that remove some component of the signal to reveal another desired component. It is effective for inferring the geology from seismic data and revealing hidden features, and gives details about the structures, lithology, stratigraphy, and reservoir properties on seismic sections **[5]** and in prediction, characterization and monitoring of hydrocarbon reservoir **[6]**. Another famous attributes are the amplitude versus offset (Avo) which is applied on data prior to stacking the traces (pre-stack filter), which could be grouped into several basic types. **[7]** divided the attributes into two general categories; geometrical and physical. The target of geometrical group is to enhance the clarity of the geometrical characters on processed seismic section which includes structure smoothing, edge evidence and variance attributes. They improve and increase the effectiveness in the identification and classification of faults and fractures in the seismic section. Physical attributes which known as stratigraphic attributes, is applied in light of the seismic facies analysis includes; relative acoustic impedance, RMS amplitude attributes, cosine-amplitude. They are playing a great role in enhancement of amplitude, phase, frequency, and related to the clarification of lithology of each formation. **[8]** Classified post-stack seismic attributes into geologic, geophysical and mathematical. The geological attributes are the most useable to get information (structural, stratigraphy and lithological properties) from the raw seismic data. Seismic attributes are controlled by components of seismic wavelet (phase; amplitude; frequency). The attributes based on phase is useful in the seismic stratigraphic interpretation (reflectors shape, geometry, continuity). The attributes based on amplitude is helpful in structural interpretations. The attributes based on frequency is very useful in evaluating reservoir properties **[5,9,10]**.

2. Geologic setting

The GOS is structurally subdivided into three tectonic provinces (Araba; Belayim; Amal), which are separated by two NE-SW oriented hinge zones (Galala-Zenima, Morgan) from north to south (**Fig. 1**). These accommodation zones are marked by significant structural discontinuities and contrasting dip regime [2,3]. Ras Gara concession (**Fig. 1)** is situated in the southern (Amal) province of the GOS which is characterized by a regional dip regime to the southwest.

Annals of R.S.C.B., ISSN:1583-6258, Vol. 25, Issue 5, 2021, Pages. 3282–3290
Received 15 April 2021; Accepted 05 May 2021

The rift-basin includes three tectono-stratigraphic sequences; the pre-rift, syn-rift, and post-rift. The pre-rift mega-unit includes Paleozoic-Upper Eocene sediments, which unconformably overlying the Precambrian basement rocks. The syn-rift mega-unit involves Oligocene-Mio. rocks, unconformably overlying the pre-rift sequences. The syn-rift sequence includes a lower predominantly clastic sequence and an upper predominantly evaporitic sequence. It comprises several source, reservoir, and seal intervals, which are associated with different structural traps. The Pliocene-Recent sediments lie unconformably on the syn-rift sequence **[11]**.

Ras Gara area is characterized by relatively thick sedimentary cover (from Late-Senonian to Recent) as derived from the drilled wells. The stratigraphic succession of the Gara Marine oil field is distinguished by thick Mio. section (> 3000 m) which includes two groups (Gharandal clastics and Ras Malaab evaporite) unconformably underlain by PM section which is characterized by reduced thickness (~500 m), and in turn overlain by sediments of the Post-Mio.

3. methodology

The ordinary steps of seismic interpretation was carried out which include; Seismic-to-well tie, Identification and distinguishing of stratigraphic boundaries; Correlation of reflectors, and Fault detection. The work begins with studying all available 2D seismic sections (15 in-lines; 14 cross-line) and wells (GMA-1, SINAI-6, SINAI-2, GMG-1, GMH-1). The time-depth relations (checkshots) of five wells are used to detect the marker horizons of Mio. age (Rudeis, Kareem, Belayim, SG and Zeit Fms). Then the formation tops posted from wells to the seismic sections to start picking horizons with fault interpretation across them. The time structure maps are calculated and contoured for each Mio. horizon. In addition, in order to get further details from the raw seismic data which is not readily apparent, the structural and stratigraphic attributes were implemented on time migrated seismic sections (in-line and cross-line). Petrel v.15 is the Schlumberger umbrella **[12]** that was used to interpret the seismic data and to generate maps.

4. Interpretation of seismic cross-sections

Figure 2A represents a composite line passing through ten migrated seismic lines from the west to east. It is evident that the quality of seismic reflectors seems to be good on tops of Zeit and SG Fms., fairly good on tops Belayim, Kareem and Rudeis Fms., bad on tops of the deeper horizons. Generally, the Gara Marine structure, as seen at Mio. level, is a SW-dipping block, which is the same regional dip regime in Amal Province. The block is terminated from the west by a major block-fault (F1) of a large vertical displacement to the east, forming a deep basinal area. Eastward, tops of the Rudeis, Kareem, Belayim Fms. are dissected by a set of NW-SE faults (F2-F8), with different throws and tilts. These normal faults seem to be inherited from deeper ones on top of basement along zones of weakness. The regional dip regime, thickness, and geometry of the Mio. strata are confirmed by a correlation chart **(Fig. 2B)** between six wells.

Annals of R.S.C.B., ISSN:1583-6258, Vol. 25, Issue 5, 2021, Pages. 3282–3290
Received 15 April 2021; Accepted 05 May 2021

5. Seismic mapping

The interpretation of seismic lines with boreholes led to construct five isochronous (TWT) maps (**Fig. 3),** are constructed on tops of Zeit, SG, Belayim, Kareem and Rudeis. They were prepared with a grid 50m*50m, showing the depth of the formation tops in terms of time (ms). Generally, the maps show a similar pattern of distribution, with time values decrease from SW to NE, and increase from top to bottom. The characteristic feature is the presence of a closure feature toward the center, which is associated with a dome-like feature. Structurally, the continuity of reflectors on tops of SG and Zeit Fms. appear to be undeformed by faults. Meanwhile, the subsalt horizons (Rudies, Kareem and Belayim) were broken by a set of NW-SE normal faults (F2-F8) of different tilts, with absence of the NE-trending faults. Westward, the structure was interrupted by a major NW-trending block-fault (F1), with a large throw to the east forming graben.

6. Seismic attributes

Seismic attributes are defined as parameters and measurements derived from seismic data such as the time, amplitude, frequency and attenuation of the seismic waves **[13]**. These attributes have long been used to provide information and details about the geologic structures, lithology, stratigraphy and reservoir properties on seismic sections **[5,10]**. Seismic attribute is any measure of seismic data that helps the geoscientist to enhance or quantify features of interpretation interest that were not possible to detect on a 3D seismic data set **[13]**. In our case, a number of first order seismic attributes were applied on two seismic lines; crossline T1084 (in NE-SW dip direction) and inline L1174 (in NW-SE strike direction). They integrated with the seismic results to enhance the structural elements, stratigraphic boundaries, and to identify new prospects.

Structure smoothing is first attribute which is applied on seismic sections to reduce/eliminate the random noises and enhance the lateral continuity of reflectors while retaining the structural details. The smooth attributes separate special seismic pattern related to certain body (such as salt structure) from other various seismic patterns (related to surroundings) in a seismic image **[14]**. Seismic data conditioning with structural smoothing before automatic interpretation produces more complete areal coverage and improves picking stability **[15]**. **Figs. 4A** and **4B** show the seismic crossline T1084 before and after conditioning by structure smoothing filter, respectively. **Figs. 5A** and **5B** display the seismic inline L1174 before and after conditioning by structure smoothing. The filtered seismic lines (**Figs. 4B, 5B**) seem to be "noise free" which is a necessary pre-conditioning step before doing other attributes. The continuity of the Mio. reflectors has been improved, and faults have been well-identified.

Edge-sensitive attributes such as coherency is a second structural attribute used to map boundaries and highlight reflectors and distinguish faults from the surroundings **[16]**. The edge content texture attribute enhances edges of geological objects in seismic image (like as any edge enhancement filter) while keeps seismic pattern and information related to other parts of the seismic image **[17]**. Coherence processing can reveal shapes of the subsurface reflectors such as unconformities, pinchouts, channel boundaries, and subtle sedimentological features which are difficult to be interpret on seismic volumes **[10]**. **Figs. 4C** and **5C** show the effect of edge

Annals of R.S.C.B., ISSN:1583-6258, Vol. 25, Issue 5, 2021, Pages. 3282–3290
Received 15 April 2021; Accepted 05 May 2021

evidence attribute after applying the smoothing attribute filter. They indicate presence of an anticlinal salt structure at top of SG Fm. The filter highlights several hairline fractures/ cracks with small throws (red lines) dissect the Mio. sections. Downward, a larger number of these cracks deform the subsalt horizons. Such a deformation may act as a conduit for hydrocarbon migration into the reservoir rocks. The deeper structure is characterized by several long faults (black lines) which grow up along zones of weakness.

The cosine of the instantaneous phase, also known as normalized amplitude, can help to enhance the definition of structural delineations. The filter is used to enhance faults, stratigraphic boundaries and to improve reflectors continuity. The presence of dense fractures in the massive rock are causing absorption effects, and led to low values of cosine instantaneous phase attributes. **Figs. 4D** and **5D** provide the same structural conclusion previously obtained from the Coherence filter**.** They exhibit the occurrence of several cracks at Mio. section that noticeably increase with depth. The Pre-salt sequence is distinguished by a set of major faults (black lines) that arisen on basement surface and vanish into the Mio. section.

Variance attribute, which measures differences from a mean value, was also applied on the seismic lines **(Figs. 4E** and **5E)**. It could be considered as an edge "coherence" method, but the variance attribute provides a more efficient results which is often sharper **[12]**. The variance was applied to detect major faults and subtle fractures that may be difficult to interpret from the original seismic lines. The faults could be assigned where the reflector end deviates from its regional dip regime. **Figs. 4E** and **5E** display two examples of variance attribute filter after doing smoothing attribute on the seismic section. The cross-line (**Fig. 4E**) is evidenced by a number of NW-trending Clysmic faults that arisen on basement surface, rejuvenated into the overlying PM section and die out into the Mio. formations. The seismic in-line (**Fig. 5E**) show no major faults cut across the sedimentary cover from bottom to top, only cracks. The filtered sections show powerful events and good continuity due to notable contrast between salt and non-salt.

Relative acoustic impendence attribute is first stratigraphic filter which used to remove or reduce low frequency noises and to map differences in impedance within layers of interest. The filter appears apparent acoustic contrast, indicates sequence boundaries, unconformity surfaces and discontinuities. It can also indicate porosity or fluid content in the reservoirs and help extract clear geologic and tectonic information. The relative acoustic impedance attributes in **Figs. 6A** and **6D** show observable contrasts between the evaporite and non-evaporitie rock units, forming a clear difference both on top and bottom. The high reflectivity could be attributing to effect of the non-porous rocks (evaporites) with intercalations of porous members (sands/shale), which led to a significant contrast of relative acoustic impedance between every two different layers. Also, the presence of high fluid content inside the reservoirs led to contrast of relative acoustic impedance. The filter reveals a domal salt structure with pinching out of the overburden Zeit Fm.

The RMS is defined as the square root of the sum of the squared amplitudes in a data set divided by the sample size of data within the time window desired. RMS attribute can aid in mapping direct hydrocarbon indicators and can also highlight other geologic features which are isolated from background features by the amplitude response. **Figs. 6B** and **6E** reveal a strong response

Annals of R.S.C.B., ISSN:1583-6258, Vol. 25, Issue 5, 2021, Pages. 3282–3290
Received 15 April 2021; Accepted 05 May 2021

(yellow color) placed at tops of Rudeis, SG and Zeit Fms. The white arrows refer to high amplitude values which are associated with abrupt changes in lithology or in fluid content and can be used as hydrocarbon indicators **[18]**. They are characterized by high energy related to rapid lithological change between shale/anhydrite at top Zeit, between shale/salts at top SG and shaly-sand/anhydrite at top of Rudeis Fm. Extra pores within the clastic rocks decrease the entire density causing a reduction of the strength of the reflected seismic waves.

Figs. 6C and **6F** sketch the effect of envelope attribute which is defined as reflection strength attribute or the total instantaneous energy of the analytic signal. The filter focuses on the lithological changes (porous-non porous zones) and sedimentary sequences boundaries as well as bright spots caused by gas accumulations. Practically, the sedimentary section is characterized by high reflectivity at salt-non salt interfaces due to the strong acoustic impedance and seismic velocity contrast. The white arrows are referring to bright spot, which considered as gas pools within the intercalated sandstone layers. The lower values (blue color) most probably are due to decrease the reflection intensity.

7. Discussion

The TWT maps on the tops of the Mio. horizons reveal a structural closure toward the center which easily correlated with the diapiric salt structure at the Upper Mio. SG Fm. The location of such a anticlinal closure at the up-thrown sides of the tilt-block is of major significance for drilling. The contacts of the salt diapir may serve as seals for the petroleum accumulations from dipping flanks/limbs.

The diapiric doming is most probably caused by the load of thick overburden (post-salt) on SG Fm, associated with reactivation of the basement faults. The ordinary seismic analyses indicate that the thickness of the Post-Mio. sediments increases toward the east and west. The conditions of salt diapir formation resulted in pinching out the Zeit Fm.

The optimal filters of seismic attributes clarify some hidden features in Mio. and PM which not clear on original seismic sections. They indicated that the Mio. section is characterized by a thick salt section, interrupted by a diapir structure at top of SG Formation. They reveal that of the Mio. section is cracked by fractures that increase with depth.

The structural seismic attributes confirm predominance of the NW-trending Clysmic faults at pre-evaporite level that developed preferentially along pre-existing lines of weakness on basement surface and stopped in Mio. section. Contrary, they exhibit a lake of the NE-trending faults, which could attribute to their geometry, due to horizontal displacements and small throws.

Stratigraphic attributes highlight strong reflections and high amplitude values at top and bottom of the Mio. evaporites the filters help identify the sequences boundaries and focus on bright spots caused by gas accumulations, which relate to rapid lithologic changes and velocity differences.

8. Conclusions

In view of the prior discussions, the ordinary seismic interpretation sees Ras Gara as a NE-SW tilted fault-block, overlain by a thick sedimentary succession. The Mio. section exhibits presence

of a salts domal feature at top of SG Fm. that overlain by a thick section of post-Mio. sediments, underlain by thinner section of PM sediments and flanked by down-stepping limbs to the east and west. Further details were obtained using the structural seismic attributes that confirm the sedimentary section is affected by a dense fracture and cracks that greatly reduced at the Mio. level. The entire of the block is affected by the NW-trending (Clysmic) faults, with absence of the NE-SW (Aqaba) faults. Stratigraphic attributes exhibit strong reflections and amplitudes on top/bottom of massive units, with pinching out the overburden Zeit Fm. They spotlight on the major lithological boundaries, and define "bright spots" which could be caused by gas accumulations.

References

[1] M. Abdel Gawad, Lithostratigraphy, A 267 (1970) 23–40.
[2] W.M. Meshref, , A.A. Blkema Rotterdame Brookfield 19, 1990, pp. 1013–1026.
[3] A.R. Moustafa, Egyptian general petroleum organization-DEMINEX, (1976) p.16.
[4] N. Sultan, K. Schutz, 7th EGPC. Explo. Semin. Cairo, (1984) p.15.
[5] M.T. Taner, Canad. Soc. Explo. Geophy. Recor, (2001) 49–56.
[6] Q. Chen, S. Sidney, Lead. Edge 16, (1997) 445–456.
[7] M.T. Taner, Attributes revisited 2000, (1992).
[8] A. E. Barnes, Handbook of Post-stack Seismic Attributes (2016).
[9] A.R. Brown, Geophysics, 66 (1) (2001) 47–48.
[10] S. Chopra, K.J. Marfurt, Geophysics, 70 (5) (2005) 3SO–28SO
[11]F. Orszag-Sperber, G. Harwood, A. Kendall, B. Purser, Chapman H, Lond., (1998) 409–426.
[12]Schlumberger, Petrel Seismic-to-Simulation Software Interpreter's Guide to Seismic Attributes. Schlumberger, Houston, (2007) p. 115.
[13]S. Chopra, K.J. Marfurt, Society of Exploration Geophysicists, (2007) p.456.
[14] Li. Xutao, C. Qilin, Wu. Chaodong, L. Huaqing, F. Yanan, Marine and Petrol. Geol., (2016).
[15] G. Fehmers, C. Hocker, Geophysics, (68) (2003) 1286-1293.
[16]K.M. Tingdahl, M. de Rooij, Geophys. Prospect, 53 (2005) 533–542.
[17] A. Mandal, E. Srivastava, Marine and Petroleum Geology, (89) (2018) 464-478.
[18] Q. Chen, S. Sidney, The Leading Edge, (16) (1997) 445-448.

Annals of R.S.C.B., ISSN:1583-6258, Vol. 25, Issue 5, 2021, Pages. 3282–3290
Received 15 April 2021; Accepted 05 May 2021

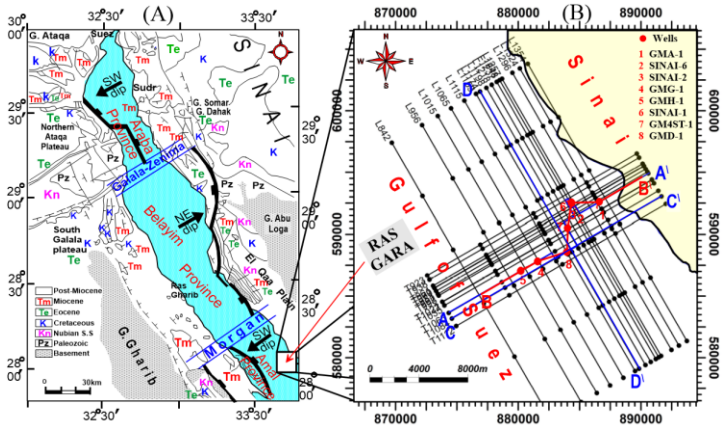

Fig. 1. a) Tectonic provinces of Gulf of Suez (modified after **[13]**), b) Ras Gara area showing shot point locations (black lines), seismic inline and crossline (blue lines), composite seismic line and correlation chart (red line).

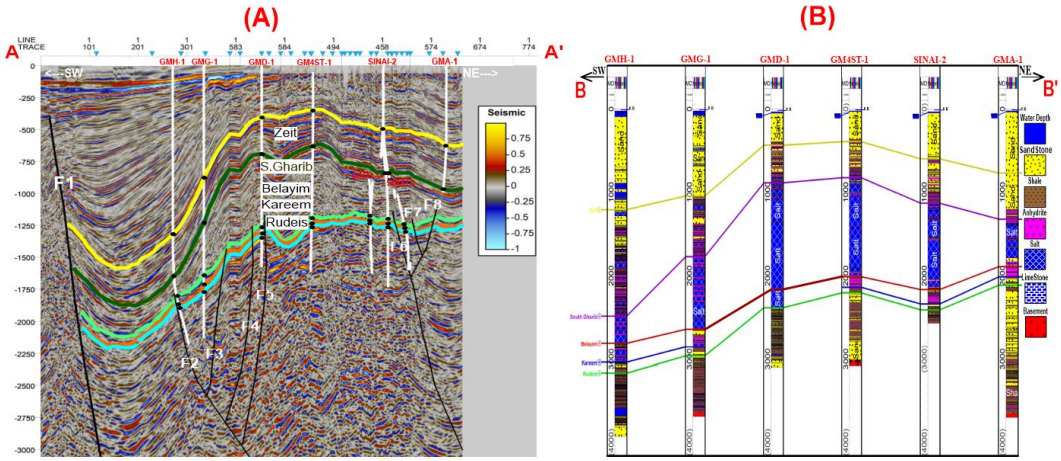

Fig. 2. A) Interpreted composite line passing throw ten seismic sections, B) Stratigraphic cross-section

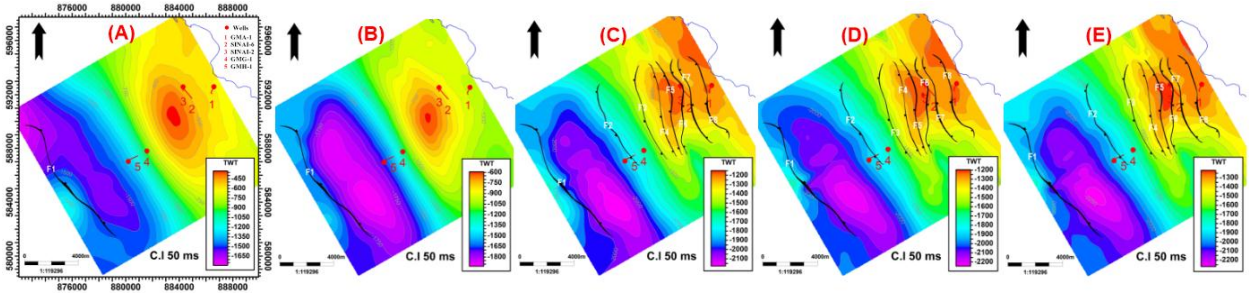

Fig. 3. Time structure maps of tops A) Zeit, B) South Gharib, C) Belayim, D) Kareem and E) Rudeis.

Annals of R.S.C.B., ISSN:1583-6258, Vol. 25, Issue 5, 2021, Pages. 3282–3290
Received 15 April 2021; Accepted 05 May 2021

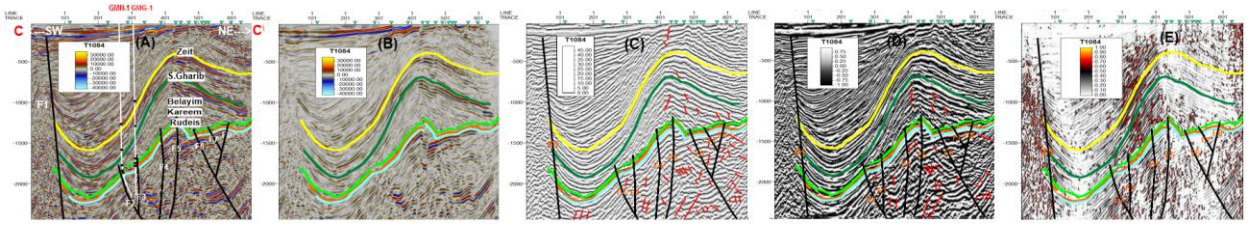

Fig. 4. Interpreted seismic crossline T1084 A) Original, B) Structure smoothing attribute, C) Edge evidence attributes, D) Cosine of phase attributes, E) Variance attributes.

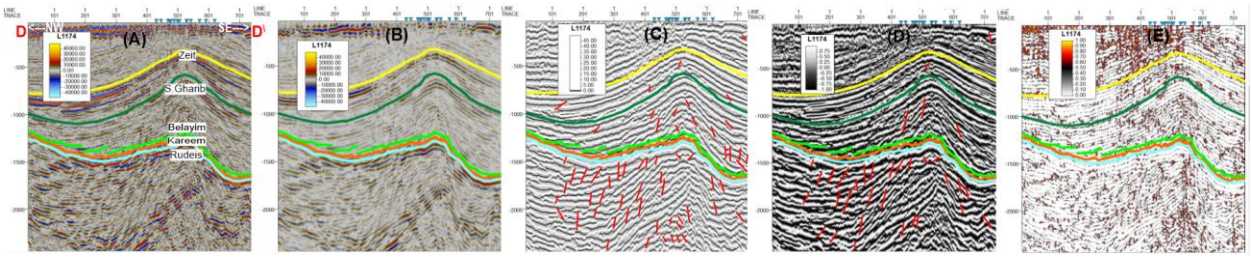

Fig. 5. Interpreted seismic inline L1174, A) original, B) Structure smoothing attribute, C) Edge evidence attributes, D) Cosine of phase attributes, E) Variance attributes.

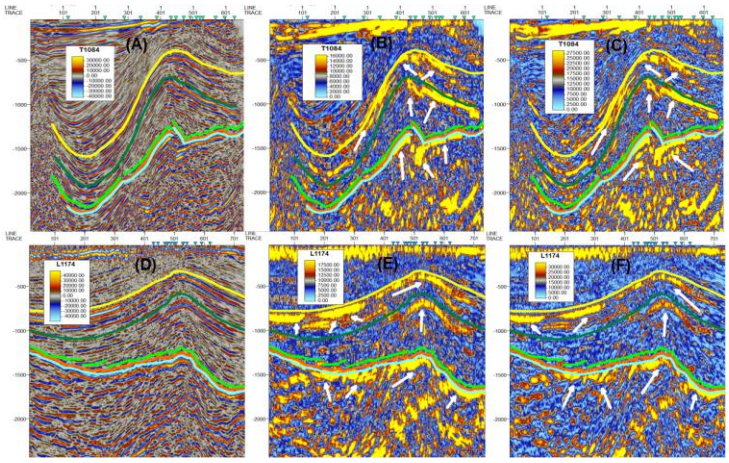

Fig. 6. Seismic crossline T1084 after applying A) Relative acoustic impedance attribute B) RMS amplitude attributes C) Envelop attributes, and seismic inline L1174 after applying D) Relative acoustic impedance attribute E) RMS amplitude attributes F) Envelop attributes.